International Journal of Thermophysics, Vol. 13, No. 2, 1992

Determination of the Thermal Conductivity of Xenon–Helium Mixtures at High Temperatures by the Shock-Tube Method

K. Hashimoto,[1] N. Matsunaga,[2] A. Nagashima,[1] and K. Mito[3]

Received July 29, 1991

The thermal conductivity of gases at high temperatures has been measured by the shock-tube method, which is uniquely suited to measure thermal conductivities of gases at high temperatures above 2000 K. A consistent set of thermal-conductivity data over a wide range of temperatures has been obtained from optimum combinations of shock-tube experiments at high temperatures, previously published data at lower temperatures, and a theoretical correlation of the temperature dependence. In the present study, the thermal conductivity of xenon–helium mixtures has been determined at compositions of 10 and 30 mol% xenon over the temperature range from 300 to 4800 K. Even though there is a large difference between the thermal conductivity of pure xenon and that of helium, it is interesting that the dependences of the thermal conductivity of the mixture on temperature and composition are linear. The experimental results are in good agreement with the predicted values based on the corresponding-states principle and the mixing rule. From these experimental results, interpolating the corresponding-states correlation data, we represent the equation of xenon–helium gas mixtures for thermal conductivity in terms of temperature and composition.

KEY WORDS: corresponding states; high temperatures; mixing rule; shock-tube method; thermal conductivity; xenon–helium mixtures.

[1] Department of Mechanical Engineering, Keio University, Hiyoshi, Kohoku, Yokohama 223, Japan.

[2] Department of Mechanical System Engineering, Takushoku University, Tatemachi, Hachioji 193, Japan.

[3] Department of Physics, Keio University, Hiyoshi, Kohoku, Yokohama 223, Japan.

0195-928X/92/0300-0211$06.50/0

1. INTRODUCTION

The xenon–helium mixture is one of the important candidates for working fluids in the SDPS (solar dynamic power system). The merits of the mixture are its high cycle performance and high thermal conductivity compared with other gases. This mixture is also interesting from a scientific point of view, since the thermal conductivity of helium is much larger than that of xenon and is suitable for testing mixing rules. From a practical and theoretical point of view, the properties of mixtures of such simple molecules are expected to be derived with theoretical methods such as corresponding states and several mixing rules. In the present study, the thermal conductivity of xenon–helium mixtures was determined over a wide temperature range by combining three separate data sources, namely, shock-tube experiments at high temperatures, critically evaluated experimental data at lower temperatures, and theoretical estimations of the temperature dependence in the intermediate range. Although the shock-tube method was extensively used in the 1960s, the results were not satisfactory. However, we consider that this method is worth using again now, since there have been major improvements in the theory and considerable progress has been made in the development of sensors and computers. Detailed descriptions of the method have been presented in our earlier publications [1, 2]. In this study, shock-tube measurements have been performed at compositions of 10 and 30 mol% xenon, where the composition dependence of the thermal conductivity is very steep, and in the temperature range up to 4800 K.

2. PRINCIPLE OF THE SHOCK-TUBE MEASUREMENTS

The theory of the shock-tube method employed in the present study has been described previously [1, 2] and is, in principle, similar to that introduced by Mastovsky and Slepicka [3]. In contrast to previous studies, in which a simple power law ($\lambda_G \propto T^n$, where n is constant) was assumed, we have derived a more exact functional form which can be used to express the temperature dependence of the thermal conductivity. The test gas (sample) bound between the reflected shock front and the end wall, at initial temperature T_1 and pressure value of P_1, is heated by compression to the temperature T_5, where it remains for about 0.5 to 1.5 ms. The pressure is raised to P_5 coincident with the temperature rise. The temperature profile at the end of the test section, developed in the initial stage at T_5, is schematically shown in Fig. 1. Since there is a large difference in the thermal conductivity between the wall material and the test gas, the temperature of the wall surface T_W is not far from the uniform

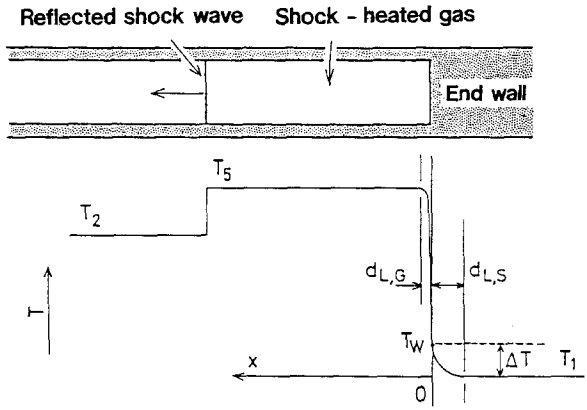

Fig. 1. Temperature profile in the test gas and in the end wall.

initial temperature T_1. It is also known that the temperature rise $(T_W - T_1)$ is practically constant throughout the duration of T_5. The temperature rise in the wall is described by the heat conduction equation.

$$\frac{\partial T}{\partial t} = a_S \frac{\partial^2 T}{\partial x^2} \tag{1}$$

where T is the temperature, t is the time, a_S is the thermal diffusivity, and x is the distance. The energy equation for the test gas is

$$\rho_G c_{P,G} \left(\frac{\partial T}{\partial t} + u \frac{\partial T}{\partial x} \right) = \frac{\partial}{\partial x} \left(\lambda_G \frac{\partial T}{\partial x} \right) \tag{2}$$

where ρ_G is the density, $C_{P,G}$ is the specific heat, λ_G is the thermal conductivity, and u is the velocity of the test gas in the x-direction. The initial and boundary conditions are as follows.

Initial condition:

$$T = T_1 \qquad (t < 0)$$

Boundary conditions:

$$T = T_W \qquad (x = 0,\ t/t_L \gg 1) \qquad \text{(test gas)}$$

$$T = T_5 \qquad (x/d_{L,G} \gg 1)$$

$$T = T_W \qquad (x = 0,\ t/t_L \gg 1) \qquad \text{(end wall)}$$

$$T = T_1 \qquad (x/d_{L,S} \ll -1)$$

$$\lambda_S \left(\frac{\partial T}{\partial x} \right)_S = \lambda_G \left(\frac{\partial T}{\partial x} \right)_G \qquad (x = 0,\ t/t_L \gg 1)$$

where t_L is the time required for the development of the temperature boundary layer and d_L is thickness of the temperature boundary layer. On the basis of the assumptions made on the temperature-independent properties of the wall material, the continuity of temperature at the wall surface, the ideal behavior of the test gas, and no radial convection, the following solution can be deduced from Eqs. (1) and (2) for the thermal conductivity of the test gas at T_5 [3]:

$$\lambda_G(T_5) = \frac{\lambda_S \rho_S c_S}{\rho_G(T_5, P_0)\, c_{P,G}(T_5)} \left[\frac{d[(T_W - T_1)(P_0/P_5)^{0.5})]}{dT_2} \right]^2 \tag{3}$$

Since $\rho_G(T_5, P_0)\, C_{P,G}(T_5)$ can readily be calculated for ideal gases, it follows from Eq. (3) that $\lambda_G(T_5)$ can be obtained by measuring $(T_W - T_1)$ and P_5 against various T_5 values. P_5 is measured with a piezo pressure gauge and T_5 is calculated either from the measurements of the shock speed or from its enthalpy. Since $(T_W - T_1)$ is monitored as the relative change in the voltage across a platinum-film sensor $\Delta E/E$, Eq. (3) becomes

$$\lambda_G(T_5) = \frac{K_W}{\rho_G(T_5, P_0)\, c_{P,G}(T_5)} \left(\frac{dF}{dT_5} \right)^2 \tag{4}$$

where

$$K_W = \lambda_S \rho_S C_S / \alpha^2 \tag{4a}$$

and

$$F = (\Delta E/E)(P_0/P_5)^{0.5} = \alpha(T_W - T_1)(P_0/P_5)^{0.5} \tag{4b}$$

As mentioned later, the apparatus constant K_W was determined by a "calibration" against the existing thermal conductivity data at lower temperatures. The resulting λ_G values are thus made free from the uncertainty in the values of λ_S, ρ_S, and C_s of the wall material. The values of F, determined over a wide range of T_5, can be obtained by varying the pressure ratio of the driver and test sections of a shock tube. Subsequently, the derivative dF/dT_5 is calculated and the value of $\lambda_G(T_5)$ is deduced with the aid of Eq. (4).

3. EXPERIMENTAL APPARATUS

The present experimental setup, schematically shown in Fig. 2, has been described elsewhere [1,2]. In the present study, the platinum-film temperature sensor was replaced with one of smaller diameter. The shock tube, 76.2 mm in inner diameter, is divided by a polyester diaphragm (3)

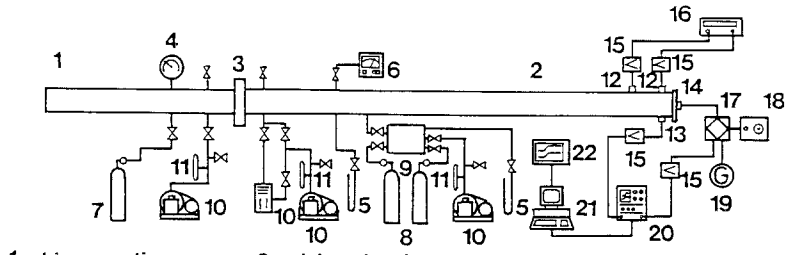

Fig. 2. Schematic diagram of the experimental setup.

into the driver (1) and test sections (2) (the length is 3 and 6 m, respectively). A Kistler 601A pressure sensor (13) monitors the pressure P_5. The shock speed is measured with a pair of piezo pressure sensors (12), fixed 0.5 m apart. The temperature rise at the wall surface is measured by a platinum-film resistance temperature sensor (14), shown in Fig. 3.

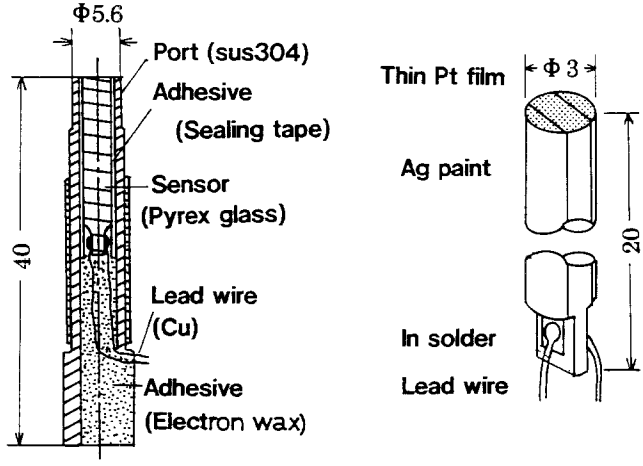

Fig. 3. Thin-film temperature sensor

The test gas of 30 mol% xenon composition was supplied by Nihon Sanso Co. Ltd. The specified composition was 29.2 mol% xenon and 70.8 mol% helium. The mixture of 10 mol% xenon was prepared by diluting the 30 mol% test gas with pure helium (specified purity, 99.995 mol%) in the mixing chamber previously described elsewhere [2]. The uncertainty in the composition of the resulting mixture was estimated as $\pm 1\%$.

4. DATA ANALYSIS

As mentioned in our previous papers [1, 2], we analyzed the results of the shock tube measurements in conjunction with critically evaluated experimental thermal-conductivity data in the range 300–1200 K. This ensured that the resulting-thermal conductivity values combine smoothly with the existing lower-temperature data. Actually, the F values for the low-temperature range were calculated from the critically evaluated data by the following equation:

$$F=\int_{T_1}^{T} \sqrt{\lambda_G(T)\,\rho_G(T, P_0)\,c_{P,G}(T)/K_W}\,dT \tag{5}$$

The F values thus obtained were then correlated with the values experimentally determined in terms of a polynomial expression temperature. Considering the temperature dependence of the thermophysical properties of dilute gases, the following functional form of F was utilized in our study [1, 2]:

$$F=k_1/T+k_2+k_3T^{0.5}+k_4T^{0.75}+k_5T \tag{6}$$

The apparatus constant K_W was determined simultaneously. In most previous studies, a power law was assumed and little attention was paid to the consistency of the temperature derivative with the data at lower temperatures. Generally, in the case of gas mixtures, one of the difficulties is the scarcity of accurate experimental thermal-conductivity data at lower temperatures. Therefore, as in the case of our previous study on argon–nitrogen and nitrogen–oxygen mixtures [2], we prepared the reference values for this temperature range by applying a mixing rule to critically evaluated thermal-conductivity data of xenon and helium. We used the data of pure xenon and helium reported by Kestin et al. [4], which were obtained by applying corresponding states to the intermolecular parameters determined from the experimental thermophysical properties of noble gases. A mixing rule for the thermal conductivity proposed by Brokaw [5] was employed in this study.

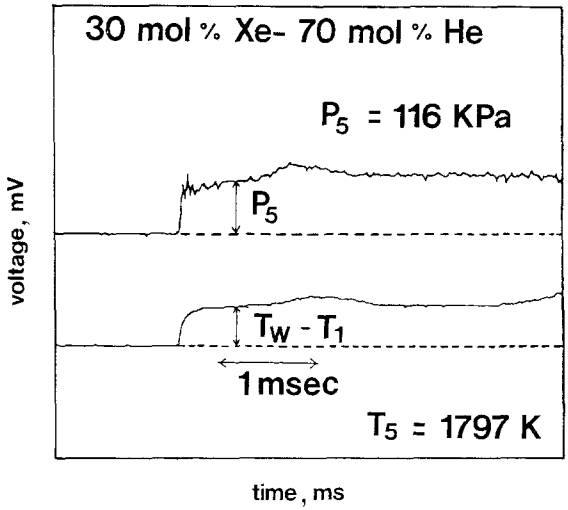

Fig. 4. Typical temperature and pressure records (70 mol% helium–30 mol% xenon).

5. EXPERIMENTAL RESULTS

The shock-tube measurements were carried out for the xenon–helium mixtures at two helium-rich compositions, namely, 10 and 30 mol% xenon. The temperature ranges of the measurements are 1500–3640 and 1400–4850 K, respectively. A typical experimental record is shown in Fig. 4.

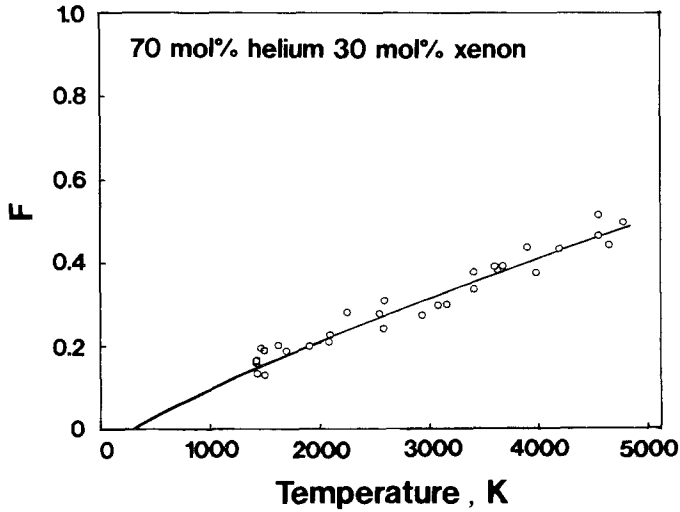

Fig. 5. F values and functions F (70 mol% helium–30 mol% xenon).

Table I. Constants for Eq. (7)

Mixture	Temperature range (K)	$10^{-4} A_1$	A_2	$10^2 A_3$
10 mol% xenon, 90 mol% helium	300–3640	10.677	7.4651	−5.7044
30 mol% xenon, 70 mol% helium	300–4850	2.9571	4.7177	−4.1193

Figure 5 is an example of F values plotted against T_5 at 30% xenon composition. In this case, the estimated uncertainty of the fit was calculated to be within ±4% in the experimental range. The thermal-conductivity values that we obtained could be represented by the following equation:

$$\lambda_G(T) = T^{0.5}(A_1 T + A_2 + A_3/T) \tag{7}$$

where λ_G is in $10^{-3}\ \mathrm{W \cdot m^{-1}}$ and T is in K.

The uncertainty to Eq. (7) including the uncertainty of the fit was estimated as ±10% for the temperature range based on the shock-tube data. The constants of Eq. (7) for each mixture are listed in Table I together with their corresponding temperature range. The thermal-conductivity values for the xenon-helium mixtures obtained in the present study are plotted in Figs. 6 and 7. These figures also show the shock-tube data of Mastovsky [9], our theoretical estimates obtained by applying Brokaw's mixing rule [5] to the thermal conductivity of each pure component based on the critically evaluated data of Kestin et al. [4]. Mastovsky measured the thermal conductivity of the xenon–helium mixtures at compositions of 10 and 50 mol% xenon in the temperature ranges 1300–6260 and 1700–7400 K, respectively. The reported uncertainty in Mastovsky's experimental data was about 10%. In Fig. 6, the thermal conductivities of

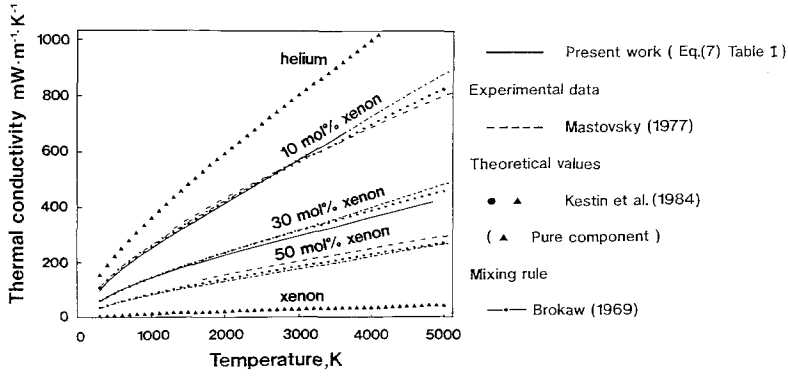

Fig. 6. Thermal conductivity of helium–xenon mixtures as a function of temperature.

the xenon–helium mixtures are shown as functions of temperature. Mastovsky's data [9] and the present results are in good agreement with the theoretiocal estimates at a composition of 10 mol% xenon. In addition, a calculation of the thermal conductivity for monatonic gases was employed using an extension of the Chapman–Enskog theory [6] to multicomponent mixtures by Kestin et al. [4]. Both Brokaw's method [5] and the correlation by Kestin et al. [4] gave practically the same results.

In Fig. 7, the present experimental and calculated thermal conductivities of the xenon–helium mixtures are compared with the experimental data of Mason and von Ubisch [7] and Gandhi and Saxena [8]; both data sets were obtained with a steady-state hot wire method. Mason and von Ubisch measured 10 binary mixtures of the rare gases and ternary mixtures of helium–krypton–xenon at 302.2 and 793.2 K. The reported accuracy of these measurements was $\pm 2\%$. Gandhi and Saxena also measured several binary and ternary systems: helium–neon, helium–xenon, neon–xenon, and helium–neon–xenon at temperatures from 303.2 to 363.2 K. The precision was reported to be $\pm 1.0\%$ with an accuracy of $\pm 2.0\%$. The composition dependences of these experimental data were reproduced with a deviation of $\pm 5\%$, in each measurement range, by both Brokaw's mixing rule and the corresponding-states principle of Kestin et al., (1985). The present experimental results show a deviation of $\pm 5\%$ in Fig. 7, compared to those calculated from the mixing rule or the corresponding-states principles. Although our data for 30 mol% xenon

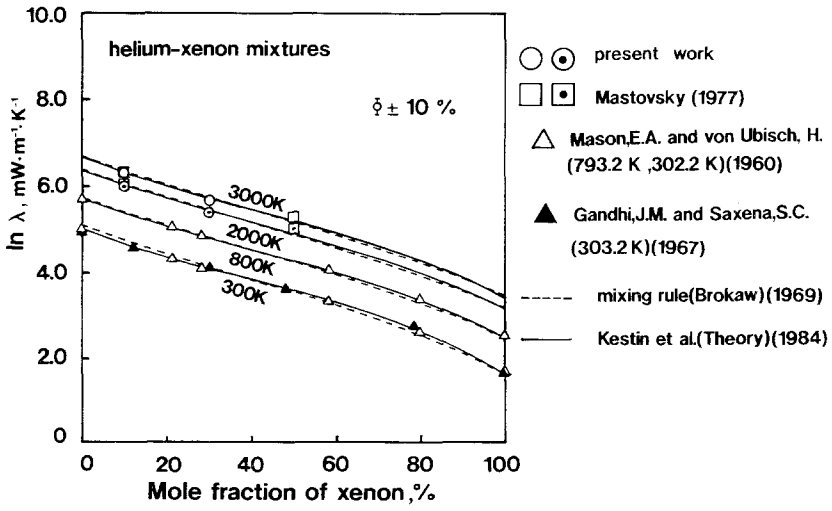

Fig. 7. Thermal conductivity in $W \cdot m^{-1} \cdot K^{-1}$ of helium–xenon mixtures as a function of composition.

Table II. Constants for Eq. (8)

$A(T)$		$B(T)$		$C(T)$		$D(T)$	
a_1	-0.0055941	b_1	0.750565	c_1	6.45997	d_1	-6047.42
a_2	-1.92121×10^{-5}	b_2	1.59642×10^{-3}	c_2	-0.454386	d_2	65.961
a_3	-4.70895×10^{-8}	b_3	6.36385×10^{-6}	c_3	-7.80966×10^{-4}	d_3	0.143214
a_4	5.16703×10^{-12}	b_4	-8.03573×10^{-10}	c_4	-1.13043×10^{-7}	d_4	-1.9280×10^{-5}
a_5	-3.88235×10^{-16}	b_5	7.04596×10^{-14}	c_5	-1.05075×10^{-11}	d_5	1.7021×10^{-9}

mixture show a weaker temperature dependence than the theoretical estimate, the discrepancy is, on the average, about 10% within the temperature range of this measurement. Mastovsky's data at an equimolar composition are about 15% higher than the predicted values and are not in agreement with our extrapolated values to lower temperatures.

On the basis of the results show in Figs. 6 and 7, the functional form of the thermal conductivity for xenon–helium gas mixtures was finally determined to be:

$$\begin{aligned}
\ln \lambda_G(X, T) &= A(T)X^3 + B(T)X^2 + C(T)X + D(T) \\
A(T) &= R^{0.5}(a_1/T^2 + a_2/T + a_3 + a_4T + a_5T^2) \\
B(T) &= T^{0.5}(b_1/T^2 + b_2/T + b_3 + b_4T + b_5T^2) \\
C(T) &= T^{0.5}(c_1/T^2 + c_2/T + c_3 + c_4T + c_5T^2) \\
D(T) &= T^{0.5}(d_1/T^2 + d_2/T + d_3 + d_4T + d_5T^2)
\end{aligned} \tag{8}$$

where T is in K and X is in mol%.

The constants of Eqs. (7) and (8) are listed in Tables I and II, and the uncertainty of Eq. (8) was estimated to be as good as Eq. (7) for each measurement temperature range.

6. CONCLUSIONS

The thermal conductivity of xenon–helium mixtures has been measured with the shock-tube method at compositions of 10 and 30 mol% xenon. The temperature ranges of the measurements are 1500–3640 and 1400–4850 K. The thermal conductivity of the xenon–helium mixtures has been expressed as a function of temperature and composition. Critically evaluated experimental data at lower temperatures were combined with and simultaneously analyzed with the present experimental results in order to obtain a consistent representation over a wide temperature range. The composition dependence of the resulting thermal conductivities showed

relatively good agreement with values calculated from a mixing rule or from the theoretical Chapman–Enskog values. The temperature dependence of the present results agree with those obtained from the theoretical estimates, in spite of the large difference in thermal conductivity of the pure components.

REFERENCES

1. T. Hoshino, K. Mito, A. Nagashima, and M. Miyata, *Int. J. Thermophys.* **7**:647 (1986).
2. K. Mito, D. Hisajima, N. Matsunaga, M. Miyata, and A. Nagashima, *JSME Int. J.* **30**:1601 (1987).
3. J. Mastovsky and F. Slepicka, *Warme Stoffübertr.* **3**:237 (1970).
4. J. Kestin, K. Knierim, E. A. Mason, B. Najafi, S. T. Ro, and M. Waldman, *J. Phys. Chem. Ref. Data* **13**:229 (1984).
5. R. S. Brokaw, *Ind. Eng. Chem.* **8**:240 (1969).
6. J. O. Hirschfelder, C. F. Curtiss, and R. B. Bird, *Molecular Theory of Gases and Liquids* (John Wiley & Sons, New York, 1954).
7. E. A. Mason and H. von Ubisch, *Phys. Fluids* **3**:355 (1960).
8. J. M. Gandhi and S. C. Saxena, *Mol. Phys.* **12**:57 (1967).
9. J. Mastovsky, *Inzh.-Fiz. Zh.* **33**:635 (1977).